

**Enhanced upper tropical tropospheric COS:
Impact on the stratospheric aerosol layer**

**J. Notholt,^{1*} Z. Kuang,² C.P. Rinsland,³ G.C. Toon,⁴ M. Rex,⁵ N. Jones,⁶ T. Albrecht,⁵
H. Deckelmann,⁵ J. Krieg,⁵ C. Weinzierl,¹ H. Bingemer,⁷ R. Weller,⁸ O. Schrems⁸**

¹ University of Bremen, D-28334 Bremen, Germany

² California Institute of Technology, Pasadena, California 91125, U.S.A.

now at: University of Washington, Seattle, Washington 98195-1640, U.S.A.

³ NASA Langley Research Center, Hampton, Virginia 23681-2199, U.S.A.

⁴ Jet Propulsion Laboratory, California Institute of Technology, Pasadena, California 91109, U.S.A.

⁵ Alfred Wegener Institute for Polar and Marine Research, D-14473 Potsdam, Germany

⁶ University of Wollongong, Wollongong, New South Wales 2522, Australia

⁷ J.W. Goethe – University, D-60325 Frankfurt/M., Germany

⁸ Alfred Wegener Institute for Polar and Marine Research, D-27568 Bremerhaven, Germany

* to whom correspondence should be addressed. E-mail: jnotholt@iup.physik.uni-bremen.de

Carbonyl sulphide (COS) is considered to be a major source of the stratospheric sulphate aerosol during periods of volcanic quiescence. We have measured the COS concentrations at the tropical tropopause and find mixing ratios 20-50% larger than assumed in models. The enhanced COS levels are correlated with high concentrations of biomass burning pollutants like CO and HCN. The analysis of backward trajectories and global maps of fire statistics suggest that biomass burning emissions transported upwards by deep convection are the source of the enhanced COS in the upper tropical troposphere.

The main sources of COS are direct emissions at the surface and the conversion of CS₂ and DMS (Dimethylsulfide) in the atmosphere (1-3). Biomass burning is assumed to contribute 10-20% to the overall source strength of COS (4-6). Due to its long lifetime, the COS mixing ratio is relatively constant throughout the troposphere at about 500 pptv (1, 7, 8) with a small decline of -0.25%/y throughout the last 24 years (9). The available data on the vertical profiles of COS exhibit no significant vertical gradient in the troposphere and a slow decrease above the tropopause (1). Much of the COS reaches the stratosphere, where photolysis and oxidation leads to SO₂ and eventually to sulphate particles (2, 4, 10). The stratospheric aerosol layer has an important impact on the radiation budget of the stratosphere, its dynamical structure, and chemistry (11). With the exception of SO₂ other sulphur compounds, such as CS₂ or dimethylsulphide (DMS), have much shorter lifetimes and are assumed not to contribute significantly to the sulphur budget in the stratosphere except during volcanic eruptions (2).

Here we present observations of COS and other related trace gases in the upper tropical tropopause region. The measurements were performed using passive absorption spectrometry in the infrared with the sun as light source (12). We discuss ground based observations performed during two Atlantic cruises onboard the German research vessel *Polarstern* where the tropics were passed in October/November 1996 and December/January 1999/2000. These observations are complemented by space borne observations above the Pacific from the ATMOS instrument flown onboard the space shuttle in November 1994.

COS and CO have been analysed between 2000 and 2200 cm⁻¹. The spectroscopic data for all molecules were taken from the most recent version of the HITRAN and ATMOS database (13). The inversion of the cruise spectra to retrieve the trace gas concentrations was implemented with SFIT2, an optimal estimation method, developed at NASA Langley and NIWA/Lauder (9). The pressure broadening of isolated spectral lines enables the determination of vertical

concentration profiles up to 30 km, with relatively coarse resolution of 4 km. The initial mixing ratios for all trace gases for the cruise analysis are based on balloon observations. For the cruise data we estimate the precision of COS and CO to be in the order of 10-15% for averaged altitude layers of 4 km (14). The ATMOS spectra have been recorded in November 1994 during sunset in occultation geometry, yielding the concentration profiles with an altitude resolution of about 1 km (15). These spectra were analysed using GFIT, a code especially developed for the analysis of balloon and satellite spectra (16). The error bars on the ATMOS vmr profiles represent their precision, which is estimated from the goodness of the fits to the measured spectra.

The cruise data from the Atlantic (Fig. 1) show an unexpected positive gradient of the mixing ratio of COS between the ground and the tropical tropopause during both cruises. Enhanced mixing ratios up to 600 pptv were found below the tropical tropopause, at altitudes between 10 and 18 km. The ship borne observations are supported by the ATMOS observations from the tropical Pacific (Fig. 2), which also reveal a COS enhancement in the upper tropical troposphere at 16 km. Although the COS enhancement of the individual profile shown is in the order of the uncertainty other ATMOS profiles close to the equator show persistently the same feature.

Numerous studies of the composition of the tropical troposphere, including observations of COS, were performed during several campaigns, e.g. PEM-West, PEM-Tropics, Safari, Trace-A (17-19). However, these COS measurements were limited to altitudes below 12 km. The only previous COS measurements in the upper tropical troposphere were reported by Leifer (20).

We suggest that the enhanced levels of COS just below the tropical tropopause are related to biomass burning. For the cruise data this assumption is supported by our observations of CO, a biomass burning product, also yielding enhanced mixing ratios in the upper tropical troposphere (Fig. 1). The ATMOS space shuttle observations of COS and CO are in agreement with the cruise

data (Fig. 2). In addition, the ATMOS spectra allow the retrieval of HCN, another biomass burning product. The mixing ratios of CO and HCN are correlated with COS, confirming that the source of the enhanced COS is biomass burning. The ratio of the COS/CO enhancement is in agreement with literature data on biomass burning emission factors of COS/CO (6, 7, 21).

The tropical troposphere above 13 km is termed the tropical tropopause layer (TTL) (22). Lower tropospheric air enters this layer in vigorous convective overshoots, then slowly ascends through the layer before fully entering the stratosphere. The ratio of the characteristic horizontal velocity ($\sim 5 \text{ m s}^{-1}$) to the global-scale mean vertical velocity ($\sim 0.5 \text{ mm s}^{-1}$) is about 10^4 near the tropopause (23). Individual localized deep convection events associated with intense fires rapidly transport pollutants into the TTL (22).

Our observations yield consistently enhanced concentrations of biomass burning pollutants in the TTL region. They suggest that pollutants from individual convective events accumulate in the TTL, are distributed zonally and chemically destroyed during slow ascent.

Both cruises traversed the tropics during periods of intense tropical biomass burning, as indicated by satellite images of the ATSR World Fire Atlas for the autumns of 1996 and 1999 (24). The ATSR data images for October 1996 and December 1999 show intense fires in Brazil and Africa. Individual backward trajectories (25) from data points within the broad region of enhanced COS originated in regions of intense burning. This is shown for two single events in Fig. 3. Trajectories cannot resolve localized deep convection events, but their rapid fluctuations in altitude close to the biomass burning plumes (see arrows in Fig. 3) suggest the presence of unresolved convection in these regions. Hence, further backward trajectory calculations would be uncertain and we terminated the trajectory calculations at the convective regions. The trajectories in Fig. 3 illustrate the transport mechanism that has been described above. The overall picture of

enhanced COS is the result of the impact of many individual events like those illustrated in the two trajectories, accumulated over the period of the burning season.

The trace gas profiles from the ATMOS instrument allow the age of an air mass since encountering combustion to be estimated by looking at the ratio C_2H_2/CO (26) (Fig. 2). Both trace gases have similar emission sources at the ground, but different reaction rates with their main sink, the OH radical. Large ratios are indicative of a young air mass and vice versa (26). The ATMOS space shuttle data show a clear maximum in that ratio at 17 km, further supporting the picture of convective overshoots of biomass burning pollutants and zonal transport in the TTL.

During the 1999/2000 cruise, CO peaks at lower altitudes than COS, consistent with chemical conversion in the TTL during the slow ascent. The lifetime of CO, governed by the reaction with OH, is shorter than that of COS, which is mainly photolysed. Furthermore, HO_x (OH + HO_2) concentrations in the upper tropical troposphere are found to be enhanced by a factor of 2-4 (27), reducing further the lifetime of CO. Hence, during ascent the ratio of CO/COS decreases. Our observations in 1999/2000 were performed 1-2 months after the main biomass-burning season. Therefore, CO at the higher levels has already been depleted.

In the lowest troposphere CO mixing ratios north of the equator were enhanced for the cruise 1999/2000, unrelated to the COS observations. Backward trajectories for December 1999 at 1.5 km altitude (25) indicate that these lower tropospheric air masses probed between 5°N and 30°N passed southern Europe. We conclude that these air masses are from industrial emissions rich in CO but not in COS.

The results indicate that at the stratospheric entry point a much larger fraction of the ambient COS comes from biomass burning events than previously thought. Comparing the maximum values of 600 pptv COS, measured at the tropical tropopause above the Atlantic, with

the 400-500 ppbv, assumed by models (28, 29), increases the contribution of COS as source for the stratospheric background aerosol layer by 20-50%. However, model calculations indicate that the production of the stratospheric aerosol layer from COS oxidation is 2-13 times smaller than required to maintain the stratospheric background aerosol layer (1, 28, 29). Recent isotopic studies of COS suggest that either COS is a minor contributor to the stratospheric aerosol layer or that current views about the ^{34}S -abundance and atmospheric circulation are seriously flawed (30).

In addition to the processes involving COS, recent findings suggest that direct emissions of gas-phase sulphate precursors and SO_2 in connection with deep convection contribute to the stratospheric aerosol formation to a greater extent than previously assumed (28, 29, 31). Pitari et al. (31) calculated that 43% of the stratospheric aerosol is formed via COS, the stratospheric SO_2 oxidation accounts for 27% and the remaining 30% is upward-transported tropospheric sulphate.

The results presented here could lead to a paradigm change in our understanding of the composition of air in the upper tropical troposphere. Our observations show that tropical biomass burning emissions have a stronger impact on the composition of the upper tropical troposphere, the entry point of air into the stratosphere, than previously assumed. The recent decline of SO_2 emissions from Europe and North America and reduced contribution to the anthropogenic component of stratospheric aerosol may have been compensated by positive emission trends of tropical biomass burning and anthropogenic SO_2 emissions from tropical and subtropical Southeast Asia (32). This might explain why SAGE II data of the stratospheric aerosol layer show no evident anthropogenic trend over the last 15 years (33).

References and Notes

1. M. Chin, D. D. Davis, *J. Geophys. Res.* **100**, 8993 (1995).
2. H. Berresheim, P. H. Wine, D. D. Davis, in *Composition, chemistry, and climate of the atmosphere*, H.B. Singh, Ed. (Van Nostrand Reinhold, New York, 1995), pp. 251-307.
3. A. J. Kettle, U. Kuhn, M. von Hobe, J. Kesselmeier, M. O. Andreae, *J. Geophys. Res.*, **107**, ACH 25 (2002).
4. M. O. Andreae, P. J. Crutzen, *Science* **276**, 1052 (1997).
5. P. J. Crutzen, L. E. Heidt, J. P. Krasnec, W. H. Pollock, W. Seiler, *Nature* **282**, 253 (1979).
6. M. O. Andreae, P. Merlet, *Global Biogeochem. Cycles* **15**, 955 (2001).
7. D. C. Thornton, A. R. Bandy, B. W. Blomquist, B. E. Anderson, *J. Geophys. Res.* **101**, 1873 (1996).
8. J. E. Johnson, A. R. Bandy, D. C. Thornton, T. S. Bates, *J. Geophys. Res.* **98**, 23443 (1993).
9. C. P. Rinsland *et al.*, *J. Geophys. Res.*, **107**, 22, ACH 24 (2002).
10. P. J. Crutzen, *Geophys. Res. Letters* **3**, 73 (1976).
11. G. P. Brasseur, J. J. Orlando, G. S. Tyndall, *Atmospheric chemistry and global change*, (Oxford Univ. Press, Oxford, 1999).
12. L. R. Brown, C. B. Farmer, C. P. Rinsland, R. Zander, in *Spectroscopy of the Earth's Atmosphere and Interstellar Molecules*, Rao, K.N., A. Weber, Eds. (Academic, San Diego, 1992), pp. 97-151.
13. L. S. Rothman, L.S. *et al.*, *J. Quant. Spectrosc. Radiat. Transfer* **60**, 665 (1998).
14. Errors in the retrieved vmr profiles can result from (i): The instrumental response function. It was measured during the 1999/2000 cruise by cell measurements with a gas of known pressure and the resulting instrumental line shape has been taken into account in the analysis. (ii): The assumed atmospheric pressure/temperature. They were measured daily onboard the ship by balloon sondes during both cruises. (iii): Initial vmr-profiles. Sensitivity tests (scaling the whole profile or shifting the profile with respect to altitude) gave similar results. (iv): The spectroscopic data: The most likely problems are the air-broadening half-widths and their temperature dependence. We have analysed spectra recorded with the same instrument in Spitsbergen in the high Arctic (79°N, 12°E, 20 m above

sea level) and at Potsdam (52°N, 80 m above sea level) in exactly the same way as the cruise spectra. At both locations the atmospheric temperatures show strong seasonal variabilities. The high latitude vmr profiles derived yield relatively constant COS mixing ratios in the whole troposphere in agreement with the available balloon observations and do not indicate erroneous spectroscopic data.

In addition to the spectroscopic remote sensing observations, CO was also measured onboard the ship during the 1999/2000 cruise by an in-situ monitor, measuring the UV resonance fluorescence of CO at 150 nm (see C. Gerbig, *et al.*, *J. Geophys. Res.* **104**, 1699, 1999). The instrument has an accuracy ± 1.3 ppbv and a detection limit of 3 ppbv (2 sigma) for an integration time of 1 s. The in-situ and spectrometric data for the lower troposphere are in excellent agreement confirming our spectroscopic observations.

15. M.R. Gunson, *et al.*, *Geophys. Res. Letters* **23**, 2333 (1996).
16. D. W. T. Griffith, G. C. Toon, B. Sen, J.-F. Blavier, A. Toth, *Geophys. Res. Letters* **27**, 2485 (2000).
17. J. M. Hoell, *et al.*, *J. Geophys. Res.* **102**, 28223 (1997).
18. J. M. Hoell, *et al.*, *J. Geophys. Res.* **104**, 5567 (1999).
19. M. O. Andreae, J. Fishman, J. Lindsay, *J. Geophys. Res.* **101**, 23519 (1996).
20. R. Leifer, *J. Geophys. Res.* **94**, 5173 (1989).
21. P. J. Crutzen, M. O. Andreae, *Science* **250**, 1669 (1990).
22. S. C. Sherwood, A. E. Dessler, *Geophys. Res. Letters* **27**, 2513 (2000).
23. J. R. Holton, A. Gettelman, *Geophys. Res. Letters* **28**, 2799 (2001).
24. *ATSR World Fire Atlas*, European Space Agency - ESA/ESRIN, via Galileo Galilei, CP 64, 00044 Frascati, Italy. <http://shark1.esrin.esa.it/ionia/FIRE/AF/ATSR/>.
25. The backward trajectories have been calculated on isentropic levels using HYSPLIT4 (HYbrid Single-Particle Lagrangian Integrated Trajectory) Model, 1997. Web address: <http://www.arl.noaa.gov/ready/hysplit4.html>, NOAA Air Resources Laboratory, Silver Spring, MD.
26. S. Smyth, *et al.*, *J. Geophys. Res.* **101**, 1743 (1996).

27. I. Folkins, P. O. Wennberg, T. F. Hanisco, J. G. Anderson, R. J. Salawitsch, *Geophys. Res. Letters* **24**, 3185 (1997).
28. E. Kjellström, *J. Atm. Chem.* **29**, 151 (1998).
29. D. K. Weisenstein, G. K. Yue, M. K. W. Ko, N.-D. Sze, J. M. Rodriguez, C. J. Scott, *J. Geophys. Res.* **102**, 13019 (1997).
30. F-Y. T. Leung, A. J. Colussi, M. Hoffmann, G. C. Toon, *Geophys. Res. Letters* **29**, 112-1 (2002).
31. G. Pitari, E. Mancini, V. Rizi, D. T. Shindell, *J. Atm. Sciences* **59**, 414 (2002).
32. N. Nakicenovic, R. Swart, Eds., *Emission scenarios 2000*, Special Report of the Intergovernmental Panel on Climate Change, (Cambridge Univ. Press, Oxford, 2000).
33. L. W. Thomason, G. S. Kent, C. R. Trempte, L. R. Poole, *J. Geophys. Res.* **102**, 3611 (1997).
34. We acknowledge the ATMOS team who acquired and processed the shuttle spectra and made them available for analysis. Furthermore, we thank the whole *Polarstern* crew for their assistance.

Figure captions

Fig. 1. Latitude transects of the retrieved volume mixing ratios of COS (left panel) and CO (right panel) for the two cruises in 1996 and 1999/2000. In addition, the thermal tropopause altitudes are given, as determined from the pressure/temperature profiles, measured by balloon sondes daily during the cruises.

Fig. 2. (A) Upper panel: Volume mixing ratio profiles of COS, CO, and HCN retrieved from solar occultation measurements recorded on November 14, 1994 above the Pacific (6°N, 151°W) by the ATMOS instrument flown on the space shuttle. **(B)** Temperature profile for these occultations determined from the ATMOS instrument and the ratio C_2H_2/CO , which is indicative of the age of the air masses (26).

Fig. 3. Backward trajectories ending at 14 km altitude (25). The lower parts of each panel show the altitude history of the trajectories in meters. The labels on the trajectories indicate zero UT. The rapid fluctuations in altitude, indicated by the arrows, suggest the presence of unresolved convection in these regions. The results of the satellite images of the ATSR World Fire Atlas (24) from October 1996 and December 1999 have been copied into the two panels.

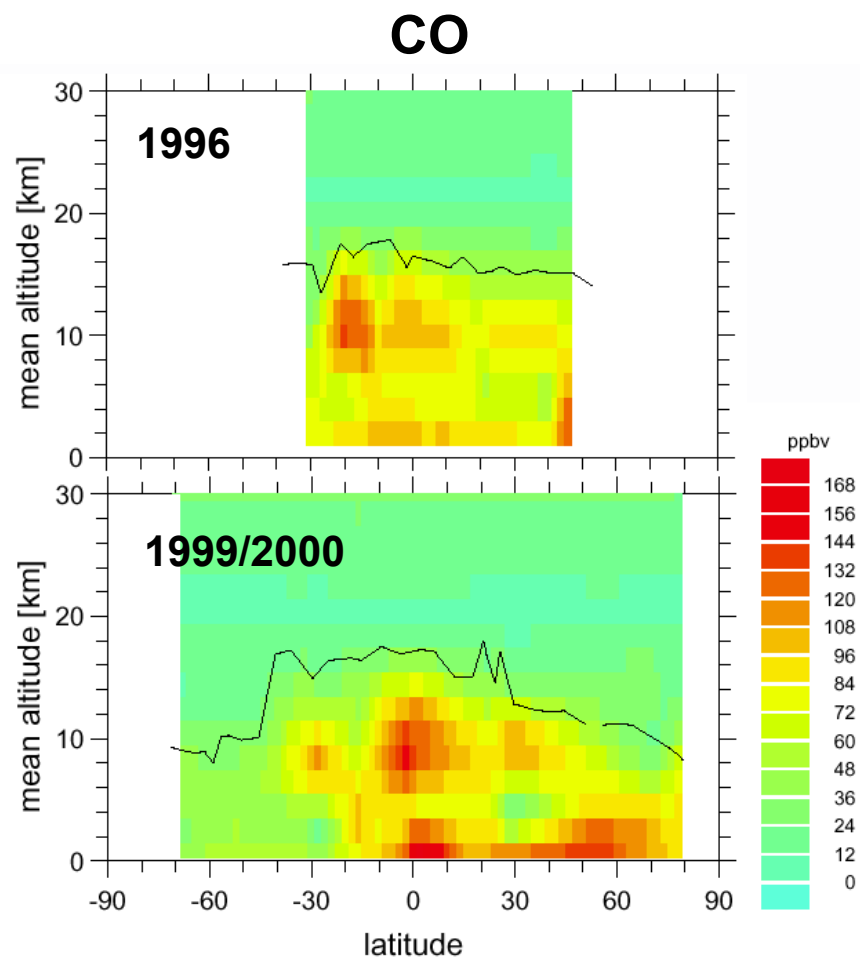
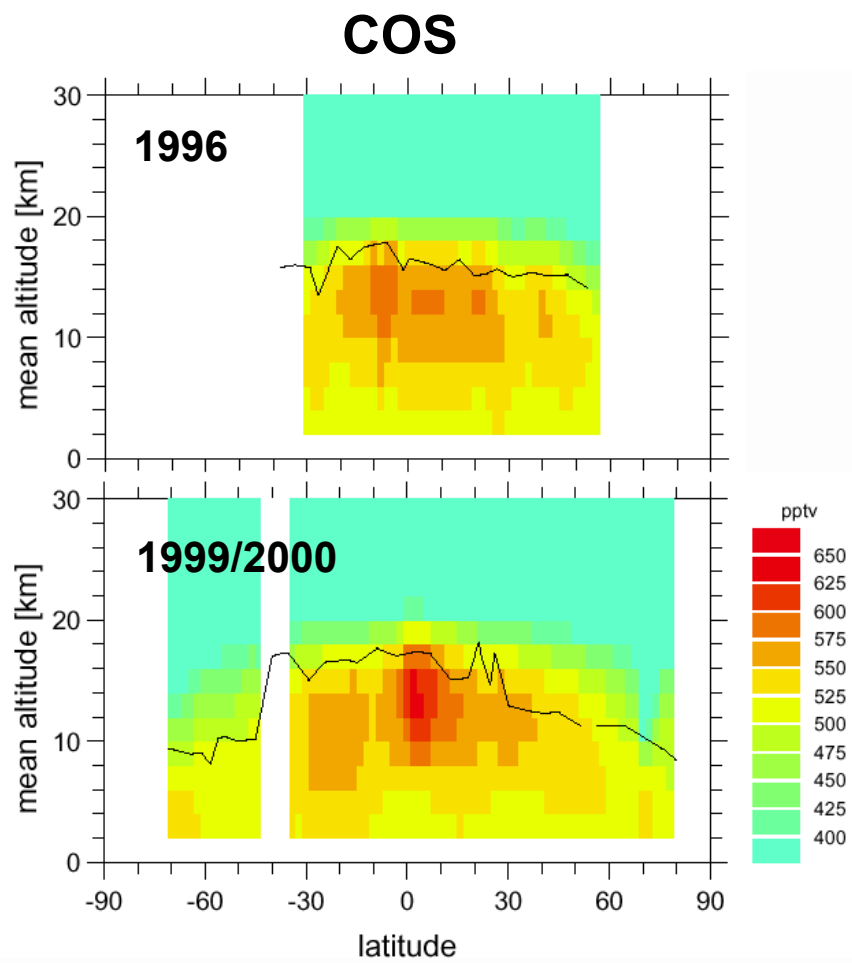


Fig. 1

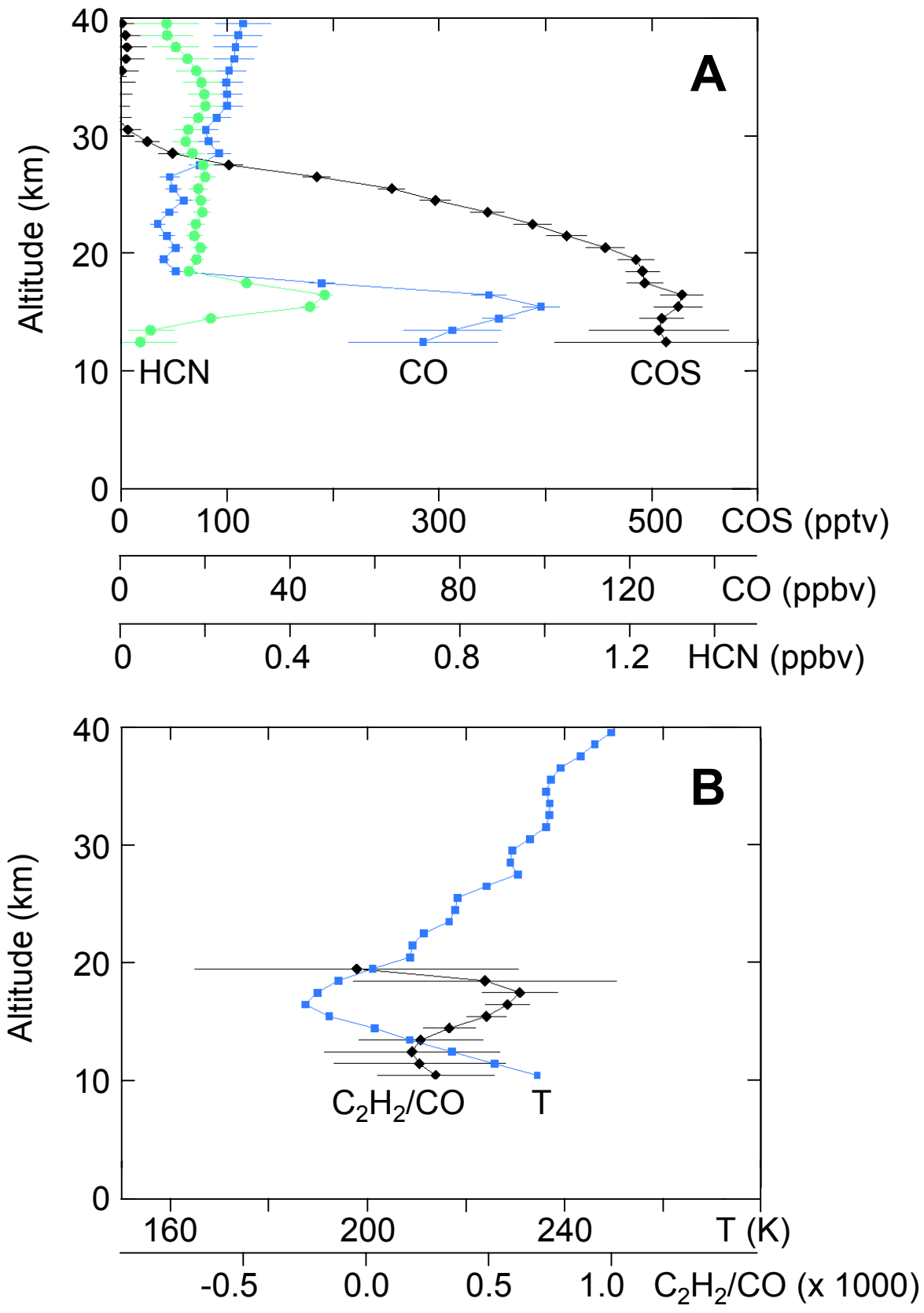


Fig. 2

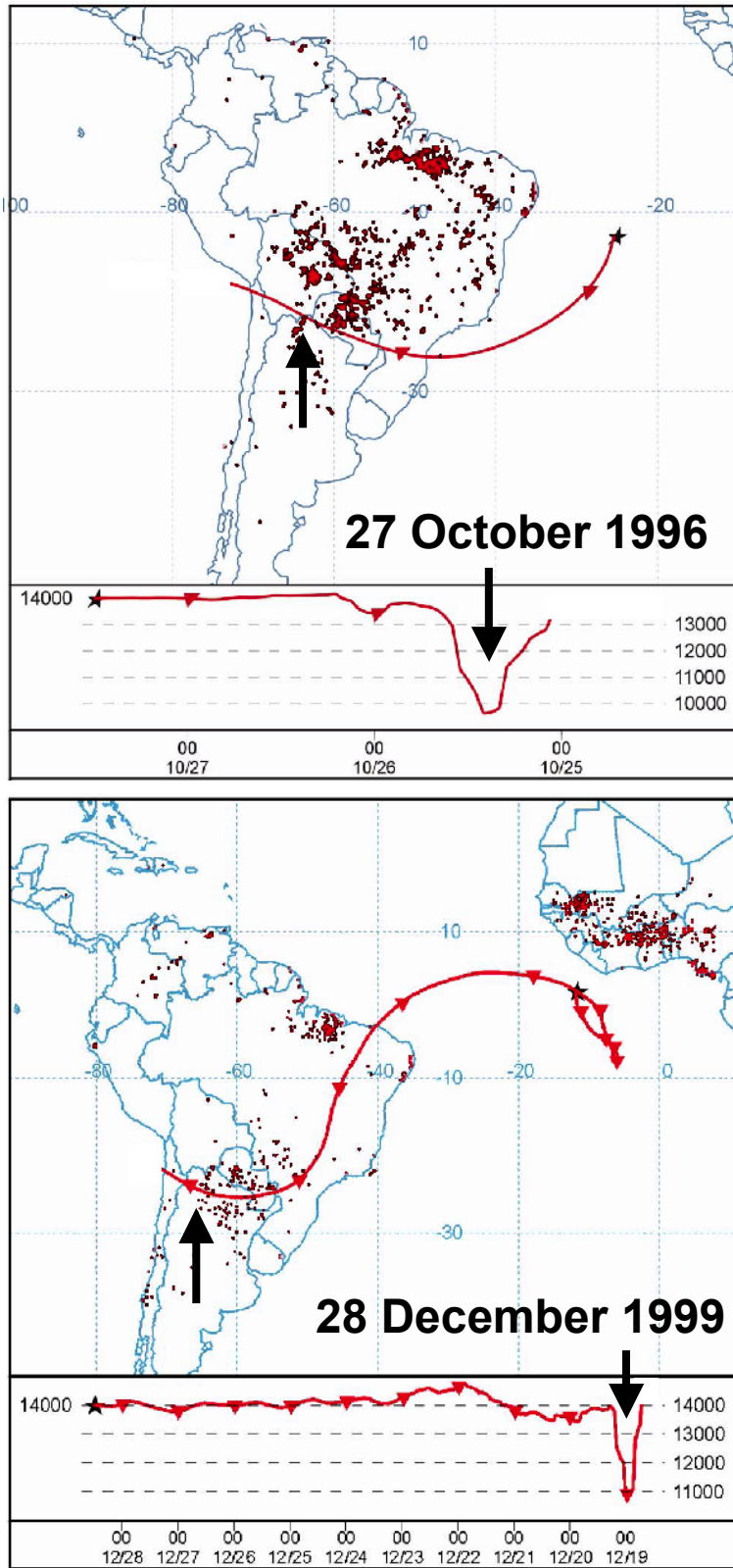


Fig. 3